



**HAL**  
open science

## An experimental investigation on the correlation between the aggregate size effect and the structural size effect

Ran Zhu, Syed Yasir Alam, Ahmed Loukili

► **To cite this version:**

Ran Zhu, Syed Yasir Alam, Ahmed Loukili. An experimental investigation on the correlation between the aggregate size effect and the structural size effect. *Engineering Fracture Mechanics*, 2020, 234, pp.107101 -. 10.1016/j.engfracmech.2020.107101 . hal-03490759

**HAL Id: hal-03490759**

**<https://hal.science/hal-03490759>**

Submitted on 3 Jun 2022

**HAL** is a multi-disciplinary open access archive for the deposit and dissemination of scientific research documents, whether they are published or not. The documents may come from teaching and research institutions in France or abroad, or from public or private research centers.

L'archive ouverte pluridisciplinaire **HAL**, est destinée au dépôt et à la diffusion de documents scientifiques de niveau recherche, publiés ou non, émanant des établissements d'enseignement et de recherche français ou étrangers, des laboratoires publics ou privés.



Distributed under a Creative Commons Attribution - NonCommercial 4.0 International License

# An experimental investigation on the correlation between the aggregate size effect and the structural size effect

Ran Zhu, Syed Yasir Alam, Ahmed Loukili

Institut de Recherche en Génie Civil et Mécanique (GeM), UMR-CNRS 6183,  
Ecole Centrale de Nantes, France.

**Abstract:** Concrete failure properties are significantly affected when the size of the structure changes. This size effect which is due to the presence of fracture process zone led by the aggregate size, has been studied in the literature only for a given concrete, however, the role of aggregate size on the size effect parameters is not clear. This paper presents an original experimental study where both the characteristic structural dimension ( $D$ ) and the aggregate size ( $d$ ) are considered as the scaling factors. The size effect is investigated by scaling of the characteristic structural dimension ( $D$ ) on three concretes, where the aggregate size ( $d$ ) is scaled with the same factor. In these concretes, the mortar content, the water/cement ratio and the aggregate content and all other mix design parameters are kept as constant. While scaling the aggregate size ( $d$ ), not just the maximum aggregate size is scaled but the complete grading curve is scaled with the same factor, which has never been done in the literature. This precise scaling of each fraction of the aggregate content in concrete and the scaling of structural dimensions reveals a direct correlation between aggregate size effect and the structural size effect parameters.

**Keywords:** concrete; aggregate size; size effect; fracture energy; fracture.

## 1. Introduction

Modelling the failure of quasi-brittle-materials like concrete and the introduction of failure mechanisms in design codes are still difficult tasks. On the one hand, this is due to the unavailability of extensive experimental data considering the effect of size, shape and boundary effects. On the other hand, it is due to the complexity of the fracture process and the heterogeneous nature of the concrete microstructure led by the aggregate size. Literature review shows several experimental studies considering the effect of size (Alam et al. 2012; Alam et al. 2014; Bažant and Pfeiffer 1987; Bažant et al. 1994; Van Vliet and Van Mier 2000; Karihaloo et al. 2003; Morel 2007), shape effects (Karihaloo et al. 2006) and boundary effects (Nallathambi et al. 1985; Duan et al. 2007). Few recent studies (Grégoire et al. 2013; Hoover et al. 2013) presented comprehensive tests where both size and shape effects are considered. These studies were mainly focused on a given concrete and the effect of heterogeneity size on fracture properties was not considered. Some work can be found in literature

(Chen and Liu 2004; Elices and Rocco 2008; Beygi et al. 2014) where maximum aggregate size was varied. However, in those studies, no correlation of the aggregate size with size independent fracture properties was developed as only the maximum aggregate size (which is usually only 10% of the complete aggregate content) was scaled, ignoring the remainder grading curve. The Structural size effect (Bažant and Planas 1998) is one of the main engineering problems for the design and prediction of failure in concrete structures; and is governed by the characteristic fracture process zone ahead of the propagating crack. Fracture process zone size is a fundamental property of concrete and is directly related to the aggregate size. It is therefore indispensable to study the correlation between the aggregate size and the structural size effect. The objective of this study is to investigate the correlation between the aggregate size and the fracture properties obtained from the size effect analysis. Three concretes are studied with same mortar content but varying aggregate size. Not only the maximum aggregate size is increased, but the complete grading curve is scaled with the same factor.

Generally, aggregate accounts for 60% – 80% of the volume and 70% – 85% of the weight of concrete of which, the coarse aggregate occupies about 45% of the volume of concrete (Neville 2011). Thus, the properties of coarse aggregate have a significant effect on the performance of concrete. Coarse aggregate properties, such as grading, surface area, particle size and shape, angularity, surface texture, mineralogy, water absorption and strength have been investigated (Aïtcin et al. 1990; Goble and Cohen 1999; Wu et al. 2001). Among these properties, maximum aggregate size ( $d_{max}$ ) is one of the important parameters that affect the properties of fresh and hardened concrete. The effect of  $d_{max}$  on mechanical properties of concrete is a complex problem. It is generally considered that coarse aggregates affect the crack propagation by crack bridging and microcrack shielding, which cause the reduction of stress in the fracture zone. Also, the interlocking of particles between the crack surfaces consumes energy and thus enhances the fracture resistance, leading to the improvement of concrete strength (Wu et al. 2001). For smaller aggregate size e.g. in case of mortar, the fracture surface is smooth. For higher aggregate size, the surface becomes rough and complex, and also some coarse aggregates are found snapped (Amparano et al. 2000; Wu et al. 2001). When maximum aggregate size is out of range, with its increase, the possibility of initial cracks to occur at the surface between coarse aggregate and matrix is increased. This surface is generally known as the interface transition zone (ITZ), which is the weakest area in concrete. With the appearance of cracks in ITZ, the bond strength of coarse aggregate is decreased, resulting in a marked decrease of the concrete strength. Basheer et al. 2005 reported that the size and porosity of ITZ increases as the aggregate size increases. Besides, the presence of microcracks may decrease if by using small aggregate size (Donza et al. 2002). In addition, crack propagation is more difficult in concrete with smaller maximum aggregate size as the mean space between aggregates is reduced (Grassl et al. 2010).

Apart from the influence on mechanical properties of concrete, aggregate size also has an impact on the fracture parameters and the brittleness of concrete.

Hillerborg (1985) showed that the maximum aggregate size affects the fracture energy ( $G_f$ ). The same results have been noticed by Nallathambi et al. (1985). While the results were not recognized by Petersson (1980) and Kleinschrodt and Winkler (1986), their results showed that the fracture energy was not affected by maximum aggregate size. Therefore, more investigations have been done by researchers to study the role of maximum aggregate size. Wolinski et al. (1987) reported that the crack surface of smaller aggregate (2-4 mm) is smoother than that of larger aggregate (8-32 mm) and there is no monotonic influence of the aggregate size on the fracture mechanics parameters. The similar results were also reported by Barr et al. (1986) for the aggregate size from 5-20 mm. Regnault and Brühwiler (1990) investigated the fracture process zone of mortar ( $d_{max} = 3$  mm) and concrete ( $d_{max} = 8$  mm). They found that the size of aggregate affects both the strain distribution and the formation of microcracks, but the fracture process zone is more pronounced in concrete than in mortar. Mihashi et al. (1991) showed that the fracture energy is significantly increased when the aggregate size becomes larger; similarly fracture process zone (FPZ) also gets wider. Besides, Mihashi and Nomura (1996) also reported that the length of fracture process zone seems to be independent of the maximum aggregate size but the width is influenced by the maximum aggregate size. However, Tasdemir et al. (1999) found that fracture energy ( $G_f$ ) and characteristic length ( $l_{ch}$ ) increase as the aggregate size is increased. While Otsuka and Date (2000) showed that the width of the fracture core zone (FCZ) and the ~~fracture process zone-FPZ~~ increase with the increase of the maximum aggregate size and the length of them shows an opposite trend. Issa et al. (2000a, 2000b) reported that the fracture energy and the fracture toughness increase with the increase of aggregate size and the fracture surface changes from smooth to rough and complex when the aggregate size increases. Same trends were also obtained by Chen and Liu (2004) and Zhao et al. (2008) for high strength concrete. Wu et al. (2001) and Chen and Liu (2007) also used acoustic emission (AE) technique to investigate the effect of maximum aggregate size. Except obtaining the similar features for fracture surfaces, the results also indicated that the fracture energy and the total number of hits increased with the increase of the aggregate size. **Improving the cement paste microstructure and packing density by replacing cement with the limestone filler also increased the fracture energy (Das et al. 2015).**

In this paper, an original experimental study is presented where both the characteristic structural dimension ( $D$ ) and the aggregate size ( $d$ ) are considered as the scaling factors. The size effect is investigated by the scaling of the characteristic structural dimension ( $D$ ) on three concretes, where the aggregate size ( $d$ ) is scaled. In these concretes; the mortar content, the water/cement ratio and ~~all-mix-design parameters~~ the total aggregate content are kept constant. While scaling the aggregate size ( $d$ ), complete grading curve is scaled with the same factor. Aggregate sizes are up-scaled in these concretes such that the volumetric fraction for each class of aggregate with respect to the maximum aggregate size (i.e.  $(d(i)/d_{max})$ ) in each concrete remains the same and is equal to the reference grading curve. Section 2 of this paper explains the materials used in this study. Specimen details and the loading

setup are presented in Section 3. Section 4 is dedicated to present the experimental results and discussion. Principal equations of the size effect method are first presented, followed by the discussion of size effect plots for each concrete. In the end, the correlation between the size independent fracture parameters and the maximum aggregate size is performed. In the light of the experimental results and the correlation, the role of the ratio between the structural size and the aggregate size is discussed.

## 2. Material properties and mix designs

Ordinary Portland cement CEM I 52.5 N is used as the binder. Water-cement ratio (W/C) is maintained to 0.4 for all the mixes. Fine aggregate is crushed fine sand with the maximum size not greater than 2 mm. Coarse aggregate is crushed limestone. Three concrete mixes are designed namely C05, C10 and C20, where the coarse aggregate size is varied. The maximum size of coarse aggregate  $d_{max}$  was taken as 5.25 mm, 10.5 mm and 21 mm respectively. Table 1 shows the mix proportion of the concretes. The three concrete mixes are designed so as to keep the same mortar volumetric proportion and properties. All the specimens from each concrete were prepared and cured in a similar way before testing. After pouring of concrete, the specimens were covered with a plastic sheet and placed in climatic room at 20°C with 95% relative humidity for 24 hours. This initial curing is to avoid the surface evaporation and autogenous shrinkage cracks. The specimens were then demoulded and kept in the climatic room at 20°C with 95% relative humidity for 28 days.

In order to scale the complete grading curve, C10 concrete ( $d_{max} = 10.5$  mm) was taken as the reference mix with the reference grading curve. The aggregate content is divided into twelve classes with respect to their size by using the ratio  $d(i)/d_{max}$ , as shown in Table 2, where  $d(i)$  is the aggregate size of the class and  $d_{max}$  is the maximum aggregate size in the complete grading curve.  $d_{max}$  is taken as 90% passing on the sieve analysis. The reference grading curve is then drawn by plotting the volumetric fraction against  $d(i)/d_{max}$  of each class. The next step is to obtain two aggregate mixes, one with  $d_{max} = 5.25$  mm (C05 concrete) and the other with  $d_{max} = 21$  mm (C20 concrete). The availability of different classes of aggregates made it possible to achieve the reference grading curve for each aggregate mix. The volumetric fraction of each aggregate class was adjusted to achieve the closest match with the reference curve. Same volumetric fraction for each class in each aggregate mix shows that aggregate is scaled by considering the complete grading curve and keeping same volumetric fraction throughout the grading curve. Table 2 shows the aggregate classes and volumetric fractions for each mix. The final grading curve of each coarse aggregate mix is presented in Figure 1.

Table 1. Mix proportion of concretes

| Concrete Series | Unit Content ( $kg/m^3$ ) |        |      |                  |             |           |
|-----------------|---------------------------|--------|------|------------------|-------------|-----------|
|                 | Water                     | Cement | Sand | Coarse aggregate |             |           |
|                 |                           |        |      | 2 – 5.25 mm      | 4 – 10.5 mm | 8 – 21 mm |
| C05             | 175                       | 439    | 772  | 926              |             |           |
| C10             | 175                       | 439    | 772  | 926              |             |           |
| C20             | 175                       | 439    | 772  | 926              |             |           |

Table 2. Coarse aggregate classes and volumetric fractions in each concrete mix

| Class $i$ | $\frac{d(i)}{d_{max}}$ | Volumetric fraction (%)            |                                    |                                  |
|-----------|------------------------|------------------------------------|------------------------------------|----------------------------------|
|           |                        | C05<br>$d_{max} = 5.25 \text{ mm}$ | C10<br>$d_{max} = 10.5 \text{ mm}$ | C20<br>$d_{max} = 21 \text{ mm}$ |
| 1         | 0.1                    | 0.0                                | 0.0                                | 0.0                              |
| 2         | 0.2                    | 0.0                                | 0.0                                | 0.0                              |
| 3         | 0.3                    | 0.0                                | 0.0                                | 0.0                              |
| 4         | 0.4                    | 8.9                                | 8.9                                | 6.8                              |
| 5         | 0.5                    | 11.9                               | 12.0                               | 11.3                             |
| 6         | 0.6                    | 19.5                               | 21.9                               | 20.5                             |
| 7         | 0.7                    | 25.8                               | 26.6                               | 27.0                             |
| 8         | 0.8                    | 15.5                               | 14.3                               | 16.4                             |
| 9         | 0.9                    | 13.3                               | 11.4                               | 13.0                             |
| 10        | 1.0                    | 4.0                                | 3.3                                | 4.1                              |
| 11        | 1.1                    | 0.6                                | 0.9                                | 0.5                              |
| 12        | 1.2                    | 0.5                                | 0.7                                | 0.4                              |

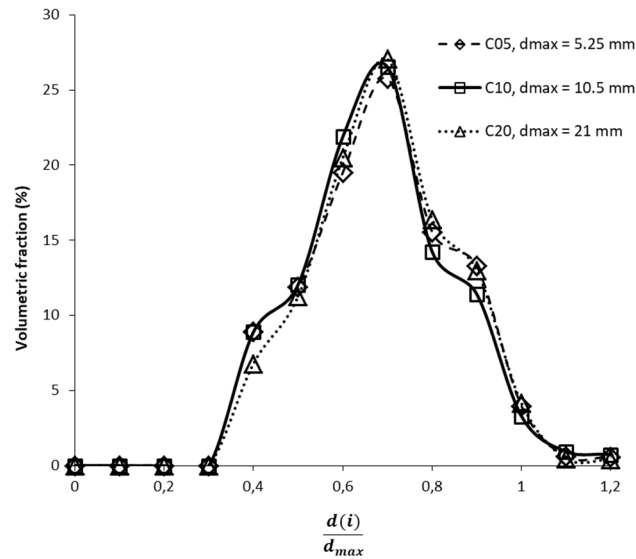


Figure 1. Coarse aggregate grading curve for each concrete

### 3. Specimens and testing procedure

Compression and Brazilian tests are carried out on each concrete using  $\phi 110 \times 220 \text{ mm}^2$  cylinders. Elastic modulus and compressive strength of the cylinders are measured according to [ASTM C469 \(2010\)](#) and [ASTM C39 \(2001\)](#) respectively. Three sets of LVDTs are used to measure the axial strains on the specimens. The static elastic modulus is defined as a chord modulus from the stress-strain curve with the first point at the strain level of 0.00005 and the second point at 40% of the maximum stress. The average mechanical properties and the corresponding standard deviations of the three specimens for each concrete and for each test are given in [Table 3](#).

Table 3. Mechanical properties of concrete mixes

| Concrete Series | Brazilian Strength (MPa) | Compressive Strength (MPa) | Young's Modulus (GPa) |
|-----------------|--------------------------|----------------------------|-----------------------|
| C05             | $3.65 \pm 0.17$          | $63.49 \pm 1.13$           | $30.40 \pm 0.18$      |
| C10             | $3.81 \pm 0.32$          | $72.97 \pm 1.03$           | $31.90 \pm 0.66$      |
| C20             | $4.19 \pm 0.49$          | $77.77 \pm 2.04$           | $33.08 \pm 0.87$      |

Three-point bending tests are performed on the concrete specimens. In order to analyse the size effect, three sizes of beams with equal width ( $b$ ) of 100 mm are designed in accordance with [RILEM-TC 89 recommendation \(1990\)](#) where the ratio of length to depth ( $L/D$ ) and span to depth ( $S/D$ ) are maintained constant. Also the ratio of the vertical notch depth to the depth of beam in all cases is equal to 0.2 ( $a_0 = D/5$ ). The experimental setup is shown in [Figure 2](#).

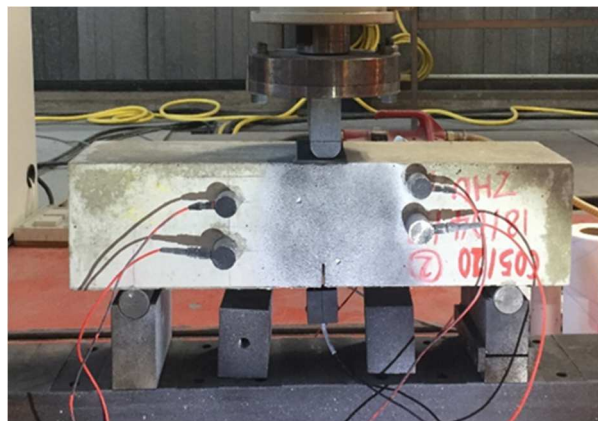


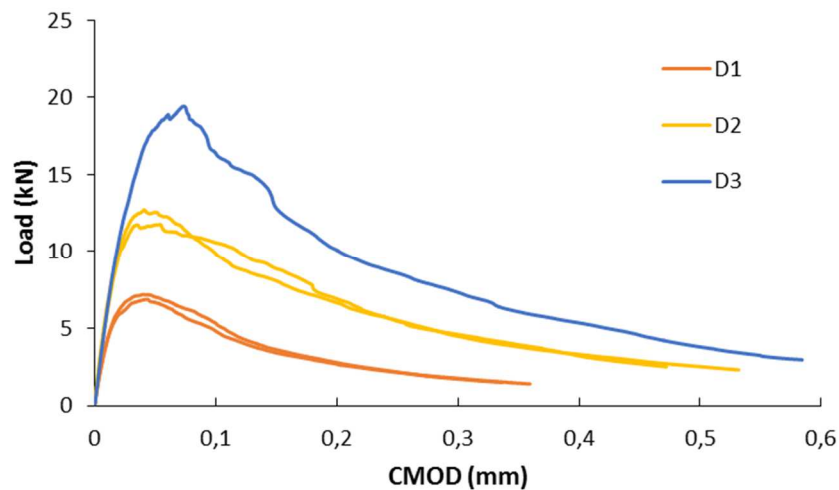
Figure 2. Experimental setup

The geometrical properties of specimens are given in [Table 4](#). It can be seen that general size effect analysis is performed on the series C05, C10 and C20 concretes using beams with depth varying from 100 mm to 400 mm. The beams are nominated as D1, D2 and D3 according to their size. Tests are conducted using 160 kN servo-hydraulic machine under closed-loop crack mouth opening displacement (CMOD) control. Bending tests are performed with a controlled crack mouth opening displacement (CMOD) rate of  $0.2 \mu\text{m}/\text{sec}$  using a CMOD clip gauge. The load and

CMOD are measured and recorded up to failure using a data acquisition system. The failure state was detected either when beam is completely broken or when the load value drops below 10% of the maximum value of the same specimen. In most cases the tests were aborted automatically by the failure of the specimens. Two beams of sizes D1 and D2, and one beam of size D3 are tested for each concrete series to consider the deviations of the results. The obtained load-CMOD curves are presented in Figure 3 and show the characteristic quasi-brittle responses of the notched concrete beams. The test duration can be calculated from the CMOD rate and final CMOD value given in Figure 3. It varies from 30 to 50 minutes depending on the size of the specimen.

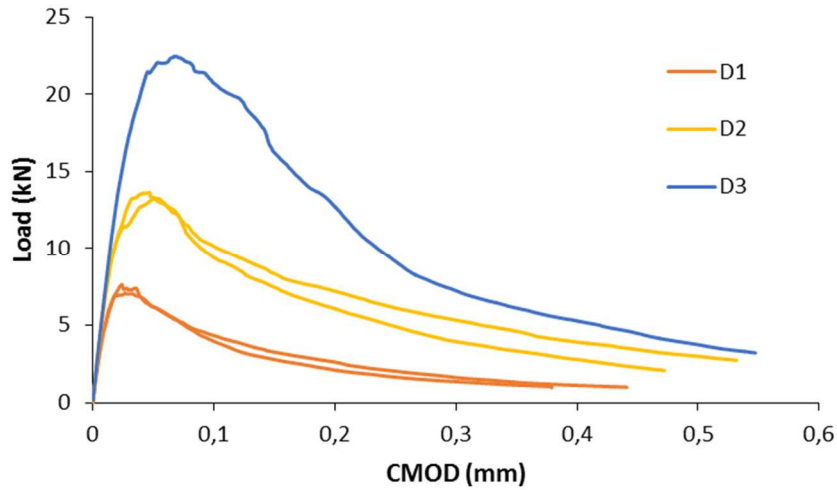
Table 4. Dimensions of specimens

| Size Nomination | Concrete Series | $D$ (mm) | $b$ (mm) | $a_0/D$ | $S/D$ | $L/D$ |
|-----------------|-----------------|----------|----------|---------|-------|-------|
| D1              | C05             | 100      | 100      | 0.2     | 3.0   | 4.0   |
| D2              |                 | 200      |          |         |       |       |
| D3              |                 | 400      |          |         |       |       |
| D1              | C10             | 100      | 100      | 0.2     | 3.0   | 4.0   |
| D2              |                 | 200      |          |         |       |       |
| D3              |                 | 400      |          |         |       |       |
| D1              | C20             | 100      | 100      | 0.2     | 3.0   | 4.0   |
| D2              |                 | 200      |          |         |       |       |
| D3              |                 | 400      |          |         |       |       |

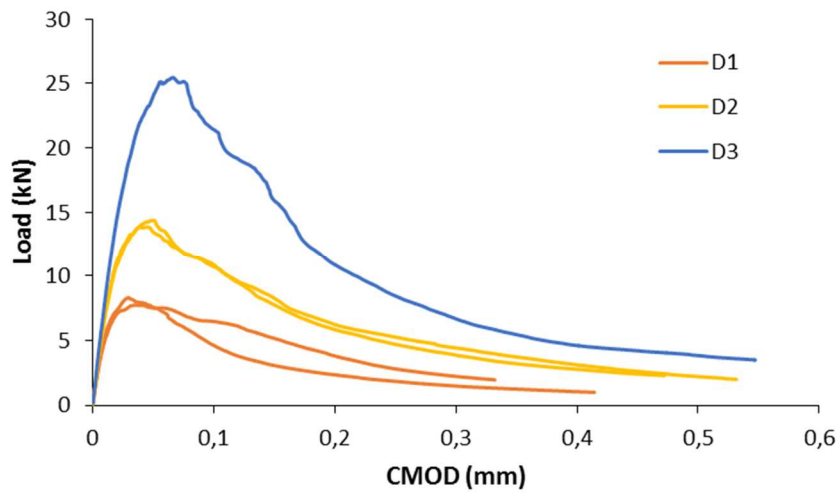


(a)





(b)



(c)

Figure 3. Load-CMOD curves of three-point bending tests for concrete series: (a) C05 (b) C10 and (c) C20.

## 4. Results and discussion

### 4.1 Structural size effect on the mechanical behaviour

Size effect is one of the most important physical phenomenon which critically impacts the mechanical and fracture behaviour of the quasi-brittle materials like concrete. As explained in Section 1, the size effect is related to the heterogeneity size of the material. Therefore, it is worthwhile to relate the size effect with the aggregate size in concrete. Bažant 1984 proposed an energetic description of the size effect based on the ductile-brittle transition of the failure modes in geometrically similar specimens. According to Linear Elastic Fracture Mechanics (LEFM), the nominal

strength ( $\sigma_N$ ) decreases in proportion to the increase of square root of depth of specimen ( $D$ ). Hence the plot of  $\log \sigma_N$  versus  $\log D$  is an inclined line with a slope of  $-1/2$ . However, in concrete structures, the size effect is transitional between the strength criterion representing horizontal line and the size effect of LEFM represented by the inclined line.

Firstly, the peak load is firstly corrected by considering the weight of beam as follows:

$$P_{max} = P_{max}^0 + \frac{2S + L}{2S} \cdot g_g \cdot m \quad (1)$$

where  $P_{max}$  is the corrected peak load,  $P_{max}^0$  is the peak load recorded by the load cell,  $m$  is the mass of specimen,  $S$  is the span,  $L$  is the specimen length, and  $g_g$  is the acceleration due to gravity.

The nominal strength is then calculated using the corrected ultimate load for each specimen using the following equation.

$$\sigma_N = \frac{3 P_{max} S}{2bD^2} \quad (2)$$

Now, Bažant (1984) size effect law can be described by the following equation.

$$\sigma_N = \frac{Bf_t}{\sqrt{1 + \frac{D}{D_0}}} \quad (3)$$

where  $Bf_t$  and  $D_0$  are empirical constants obtained by fitting the plots between the nominal strength ( $\sigma_N$ ) and the size ( $D$ ) of geometrically similar specimens.  $D_0$  is also considered as the transitional structural dimension between the plasticity and the LEFM.  $Bf_t$  is related to the strength of the structure when  $D$  approaches to zero (Bažant and Planas 1998).

Linear regression between the nominal stress and the size of specimen allows determining coefficients  $Bf_t$  and  $D_0$  in Equation 3 as follows:

$$Y = AX + C \quad (4)$$

$$X = D; Y = \left(\frac{1}{\sigma_N}\right)^2; D_0 = \frac{C}{A}; Bf_t = \frac{1}{\sqrt{C}} \quad (5)$$

Based on the concept of the equivalent elastic LEFM proposed by Bažant and Kazemi (1991) and Bažant and Planas (1998), two major fracture parameters, the fracture energy ( $G_f$ ) and the effective length of process zone ( $c_f$ ), can be determined through:

$$G_f = \frac{(Bf_t)^2 D_0 g(\alpha_0)}{\tilde{E}} \quad (6)$$

$$c_f = \frac{g(\alpha_0)}{g'(\alpha_0)} \cdot D_0 \quad (7)$$

where  $\tilde{E} = E/(1 - \nu)$ ,  $E$  is the elastic modulus of concrete,  $\nu$  is the poisson ratio,  $g(\alpha_0)$  is the non-dimensional energy release rate, and  $g'(\alpha_0)$  is the derivative of  $g(\alpha_0)$  with respect to the relative initial crack length  $\alpha_0 = a_0/D$ .

The nominal stress for each beam is presented on the size effect plot for each concrete as shown in Figure 4. The results show a transitional behaviour for each concrete and is well described by the Bažant size effect law. The quality of linear fitting and size effect plots are calculated by comparing the experimental results with regression results. The percentage errors are given in Table 5.

The parameters  $Bf_t$  and  $D_0$  obtained for each size effect plot are given in Table 5. The parameter  $Bf_t$  is almost the same for all concretes i.e. it is not affected by the size of aggregate.

Although the parameter  $D_0$  is different for each series of concrete, the obtained size effect plot is unique. All the size effect plots of Figure 4 are transferred to Figure 5, where one can analyse the combined effect of aggregate size. The quality of linear fitting and size effect plots are calculated by comparing the experimental results with regression results. The percentage errors are given in Table 5. It can be seen that with the increase of aggregate size, the behaviour approaches the hypothesis of strength criterion and with the decrease of aggregate size, the behaviour approaches the LEFM. It means that when the heterogeneity size in a quasi-brittle material like concrete is small enough as compared to the size of the structure, the material behaviour becomes brittle and can be described by the fracture mechanics principles. Since the aggregate size ( $d$ ) directly affects the fracture process zone length ( $c_f$ ), it can be inferred that in the size effect tests, the strength is in fact affected by the ratio between the characteristic structural dimension and the aggregate size ( $D/d$ ). However, if both the structural size and the aggregate size increases at the same time so as to keep the ratio  $D/d$  same, there is no effect on the nominal strength. It can be seen in Figure 5. by observing the results of D1-C10 beams and D2-C20 beams. Similar observation can be made on the results of D1-C05 beams, D2-C10 beams and D3-C20 beams. The same observation can also be made on D2-C05 and D3-C10 beams.

It can be seen in Figure 5 that the size effect on the nominal strength is very pronounced for C05 concrete where smaller aggregate is used. However, the size effect is comparatively less pronounced in the concrete mixes with larger aggregate sizes. This is expected as the material behaviour transits towards LEFM where the heterogeneity size decreases with respect to the specimen size.

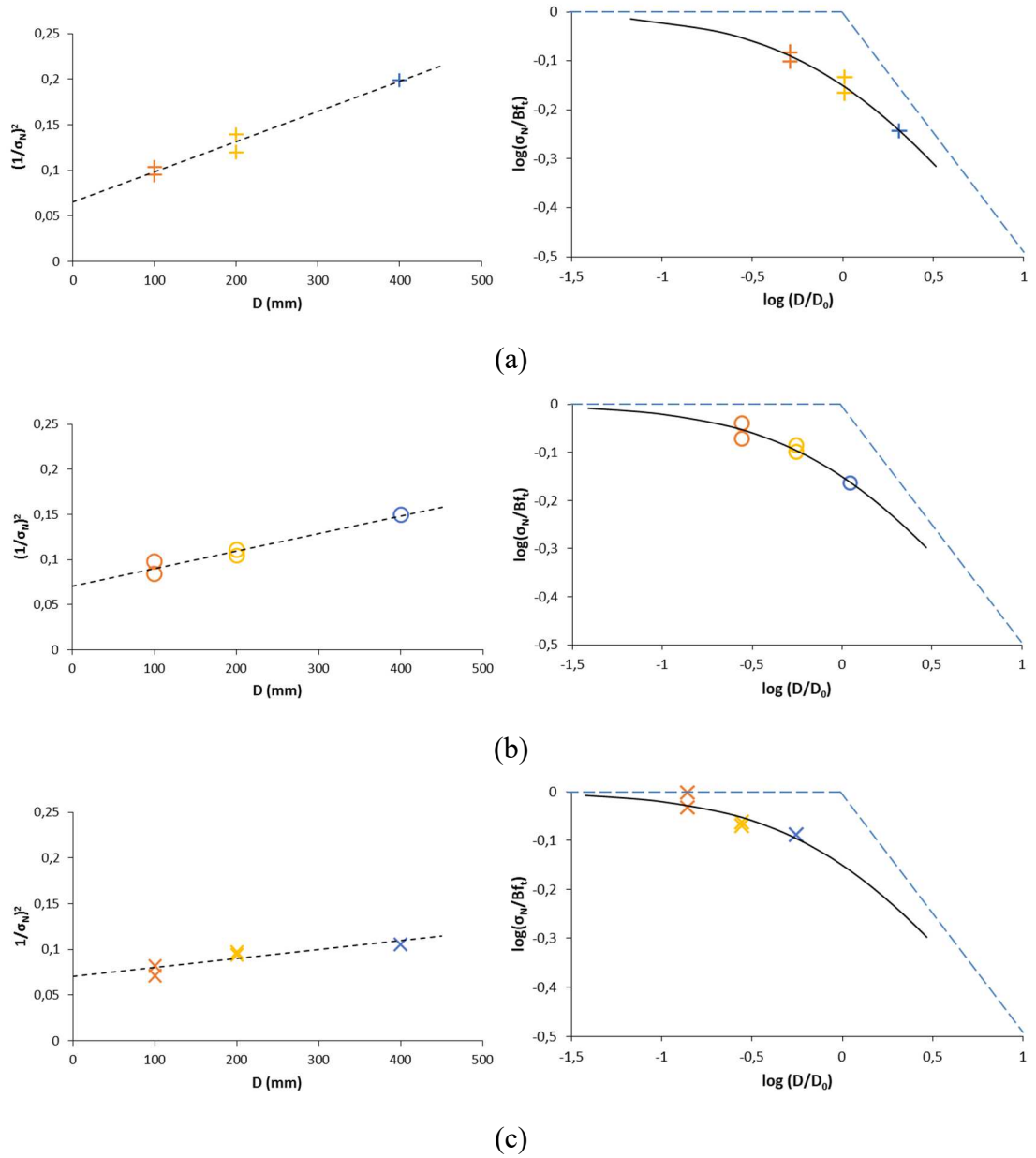


Figure 4. Size effect law for curves for concrete series: (a) C05; (b) C10; (c) C20

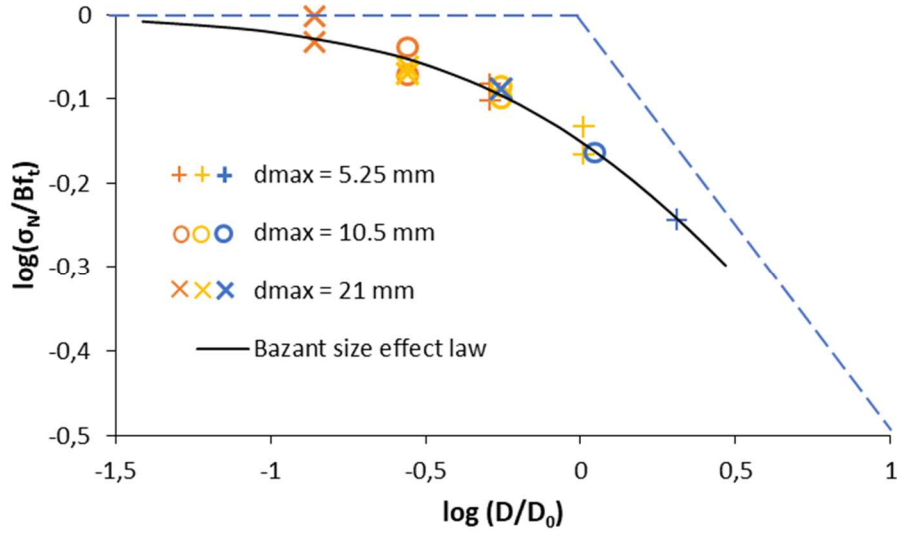


Figure 5. Combined size effect curve for C05, C10, and C20 concrete series.

Table 5. Quality of Linear regression and SEL fit measures

|                   | %age difference between experimental results and regression plots |      |         |     |         |      |                      |     |
|-------------------|---|------|---------|-----|---------|------|----------------------|-----|
|                   | C05   |      | C10     |     | C20     |      | Combined Size effect |     |
|                   | Average   | Max  | Average | Max | Average | Max  | Average              | Max |
| Linear regression | 6.0   | 10.4 | 4.4     | 7.7 | 6.0     | 13.2 | -                    | -   |
| SEL curve         | 2.4   | 4.5  | 2.2     | 4.3 | 2.9     | 5.9  | 3.0                  | 8.2 |

#### 4.2 Influence of the aggregate size on the size independent fracture properties

It can be seen from Table 5, that effective fracture process zone length ( $c_f$ ) is increased by increasing the maximum aggregate size. It means that the concrete with smaller coarse aggregate will have shorter fracture process zone than that with larger coarse aggregate. In fact, the concrete with larger aggregate contains more weakened ITZ and relatively more deviation in the cracking path (Amparano et al. 2000; Wu et al. 2001). Thus, when the maximum aggregate size becomes smaller, the effect of bridging and the aggregate interlocking (which increases the fracture process zone size) in the crack path is attenuated. Similar increase in the transitional structural dimension ( $D_0$ ) between the plasticity and the LEFM can be observed.

The relationship of  $c_f$  and  $D_0$  with  $d_{max}$  is linear and can be expressed as:

$$D_0 = n_1 d_{max} \quad (8)$$

$$c_f = n_2 d_{max} \quad (9)$$

where  $n_1$  and  $n_2$  are empirical constants and assumed to be independent of the size of

aggregate. The relationship from above equations and the experimental results are presented in Figure 6. The relationships are in very good agreement with the experimental results. The constants  $n_1$  and  $n_2$  obtained from the regression analysis are given in Table 6.

From Figure 6 it can be seen from extrapolation of linear regression that both  $c_f$  and  $D_0$  reduce to zero as the material heterogeneity size approaches to zero, which shows that  $c_f$  and  $D_0$  are in fact material parameters and are directly related to the heterogeneity size. As the heterogeneity size increases, these material parameters also increase with the same ratio. When the heterogeneity size reduces to zero, the equivalent length of the fracture process zone ( $c_f$ ) also reduces to zero i.e. no fracture process zone occurs and the material fails due to sudden crack propagation at the peak load. Similarly, when the heterogeneity size reduces to zero, the transitional structural dimension  $D_0$  also reduces to zero i.e. no transition from LEFM to Strength based law is possible if the size of structure changes.

Table 6. Size effect parameters and fracture properties from size effect analysis

| Parameters     | Concrete series |       |       |
|----------------|-----------------|-------|-------|
|                | C05             | C10   | C20   |
| $d_{max}$ (mm) | 5.25            | 10.5  | 21.0  |
| $D_0$ (mm)     | 195.6           | 360.5 | 720.7 |
| $Bf_t$ (MPa)   | 3.93            | 3.77  | 3.77  |
| $c_f$ (mm)     | 35.3            | 65.0  | 130.0 |
| $G_f$ (N/m)    | 58.4            | 94.7  | 182.5 |

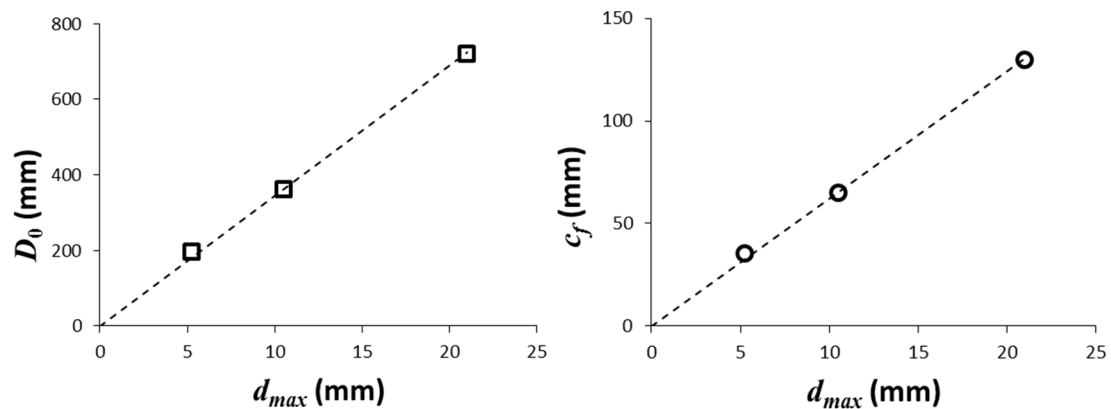


Figure 6. Variation of size effect parameters  $D_0$  and  $c_f$  with maximum aggregate size ( $d_{max}$ )

The fracture energy ( $G_f$ ) also increases with the increase of maximum aggregate size ( $d_{max}$ ). This is obvious because during the process of crack propagation, microcracking and matrix-aggregate debonding consume considerable energy. Since the increase of aggregate size causes an increase in the crack area, the energy demand required for the crack growth will also increase. The same tendency for the fracture toughness and the fracture energy has been observed in previous researches (Strange and Bryant 1979; Nallathambi et al. 1984; Rao and Prasad 2002). Jenq and Shah (1985) reported that when  $d_{max}$  increases from 4.75 to 19 mm,  $G_f$  (determined using equivalent LEFM approach) increases from 21.1 N/m to 35.4 N/m for normal concrete. Rao and Prasad (2002) found that for high-strength concrete, when  $d_{max}$

increases from 4.75 to 20 mm,  $G_f$  (determined using RILEM work of fracture method) increases from 76.6 to 142 N/m. Karamloo et al. (2016) also obtained similar results for self-compacting lightweight concrete with w/c of 0.35 and 0.4; the study showed that when  $d_{max}$  increases from 9.5 to 19 mm,  $G_f$  (determined using size effect method) increases from 25.5 N/m to 36.3 N/m and 16.9 N/m to 31.5 N/m. Few power scaling equations have been proposed in the literature (Trunk and Wittmann 1998, Beygi et al. 2014). As said in Section 1, in previous studies, the scaling of aggregate size was only done for  $d_{max}$  and did not consider the complete grading curve. Therefore, the true effect of scaling of aggregate size in a concrete mix could not be estimated. Figure 7 shows that the effect of aggregate size can be described by a linear relation between the maximum aggregate size and the fracture energy as follows:

$$G_f = A_1 d_{max} + C_1 \quad (10)$$

where  $A_1$  is the slope of the curve and  $C_1$  is the intercept at y-axis when  $d_{max}$  reduces to zero. The value of  $A_1$  obtained is equal to 7.94. The intercept  $C_1$  represents approximately the fracture energy of cement paste i.e. where the heterogeneity size is extremely small (size of cement clinker). The value of  $C_1$  obtained is equal to 14.5 N/m. The value is ~~very similar compared~~ comparable to the values in literature for fracture energy of cement paste. Coopamootoo and Masoero (2018) found the fracture energy equals to 8.3 N/m for cement paste with W/C ratio of 0.34. Xu and Zhu 2009 found the fracture energy equal to 18.3 N/m for cement paste with W/C of 0.4. Luković et al. 2015 found the fracture energy in the range of 5-10 N/m for cement paste with W/C of 0.4.

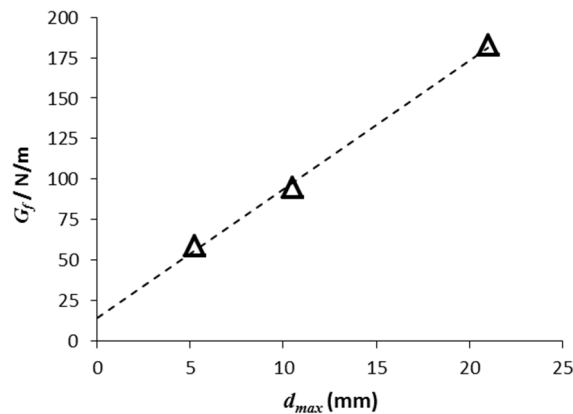


Figure 7. Relationship between the fracture energy and the maximum aggregate size

It should be noted that the relation (Equation 10) between the fracture energy and the aggregate size, would predict the same effect in all ranges of the aggregate sizes. This should be verified by testing the concrete with aggregate size range  $d_{max}$  greater 21 mm and smaller than 4 mm having same mortar properties and the aggregate grading properties. Similarly, the mix designs other than the one used in this study should also be tested. A wide range of experiments is thus needed where scaling of complete grading curve should be done for various mix designs of concretes. This paper presents only one such study with  $d_{max}$  variation from 5.25 – 21 mm, which is

the most commonly used  $d_{max}$  in concrete mix design.

In order to investigate the effect of aggregate size and the structural dimension, brittleness number  $\beta$  (Bažant and Kazemi 1990) is investigated. The expression of brittleness number can be given as:

$$\beta = \frac{g(\alpha_0) D}{g'(\alpha_0) c_f} \quad (11)$$

Figure 8 shows the variation of  $\beta$  as a function of specimen size. It can be seen that all the data is located in the range of nonlinear fracture mechanics ( $0.1 \leq \beta \leq 10$ ). The failure should be analysed according to LEFM when  $\beta > 10$  and the method of analysis approaches strength criterion when  $\beta \leq 0.1$  as reported by Bažant and Kazemi (1990).

It can be seen in Figure 8 that  $\beta$  increases as the specimen size increases i.e. the behavior becomes more brittle. The relation between  $\beta$  and the specimen size can be represented by a linear regression curve. Moreover,  $\beta$  decreases as the aggregate size increases. Also the slope of regression curve between  $\beta$  and the specimen size decreases with the increase of aggregate size. It can also be seen that specimen D1-C10 has the same brittleness number as the specimen D2-C20. Similarly, specimens D1-C05, D2-C10 and D3-C20 have the same brittleness number. From the above analysis, it can be concluded that increasing the size of specimen or decreasing the aggregate size with the same factor has similar effect on the brittleness number. If the ratio between specimen size and aggregate ratio is kept constant, one would obtain the same brittleness number.

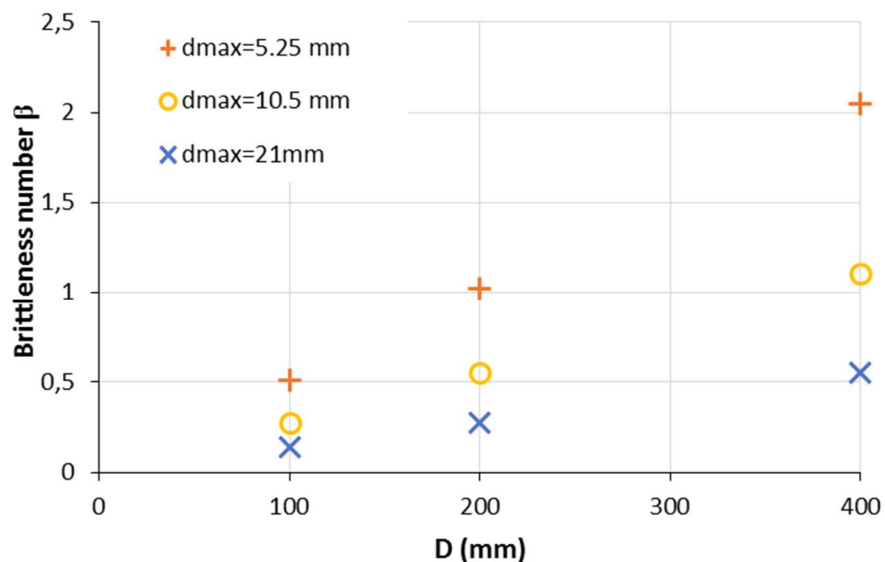


Figure 8. Variation of brittleness number with specimen size for each concrete series



## 5. Conclusion

The paper presented an experimental study to investigate the role of aggregate size on **the** structural size effect. Three concretes with increasing aggregate size were studied. Not only the maximum aggregate was up scaled, the complete grading curve was up scaled with the same scaling factor. Size effect experiments using **2D** geometrical similar three point bending specimens with central notch were performed on each concrete. The main conclusions are following:

- Upscaling the aggregate size has a significant effect on the size effect curve. The size effect reduces and the behavior approaches strength criterion when aggregate size is increased. Same size effect curve is obtained for all concretes, only the points are shifted towards strength criterion when aggregate size increases and the points are shifted towards LEFM when aggregate size is decreased. Bazant's size effect well predicts the behavior of all concretes.
- The length parameters of size effect analysis ( $c_f$  and  $D_0$ ) are linearly proportional to the maximum aggregate size ( $d_{max}$ ). The extrapolation of results shows that both  $c_f$  and  $D_0$  reduces to zero as aggregate size approaches zero. It means that  $c_f$  and  $D_0$  are material parameters and are directly related to the heterogeneity size (aggregate size). When the heterogeneity size reduces to zero, the effective length of fracture process zone  $c_f$  also reduces to zero i.e. no fracture process zone occurs and the material fails due to sudden crack propagation at peak load or LEFM.
- The fracture energy ( $G_f$ ) also increases linearly with the increase of maximum aggregate size ( $d_{max}$ ). It is found that by increasing  $d_{max}$  to four times (from 5.25 to 21 mm), the fracture energy increases from 58.4 N/m to 182.5 N/m (slightly less than four times). The increase is thus not with the same factor as aggregate size. ~~By extrapolation, it is observed that the fracture energy is approximately 14.5 N/m when  $d_{max}$  approaches to zero. This may be attributed to the fracture energy of cement paste where size of heterogeneity is very small as compared to the size of specimen.~~
- The brittleness number increases as the aggregate size decreases. Also the slope of brittleness curve increases as the aggregate size decreases. It means that when **the** aggregate size decreases, not only the brittleness increases, but its effect while changing the structural size becomes more detrimental and **the** specimen becomes more and more brittle.
- It can be observed that beams with same specimen size to aggregate size ratio have same brittleness number. This can also be observed on the size effect plot. If both structural size ( $D$ ) and aggregate size ( $d$ ) increase at the same time so as to keep the ratio  $D/d$  same, there is no effect on the nominal strength e.g. the results of D1-C05 beams, D2-C10 beams and D3-C20 beams. Similar observation can be made on the results of D1-C10 beams and D2-C20 beams. Also on D2-C05 beams and D3-C10. It means that the ratio of structural size and aggregate size is a key parameter which causes the structural size effect and the brittleness in concrete.

## 6. References

Amparano FE, Xi Y, Roh YS. Experimental study on the effect of aggregate content on fracture behavior of concrete. *Engineering Fracture Mechanics* 2000; 67(1):65-84.

Alam SY, Loukili A, Grondin F. Monitoring size effect on crack opening in concrete by digital image correlation. *European Journal of Environmental and Civil Engineering* 2012; 16(7):818-836.

Alam SY, Saliba J, Loukili A. Fracture examination in concrete through combined digital image correlation and acoustic emission techniques. *Construction and Building Materials* 2014; 69:232-242.

ASTM C469, "Standard Test Method for Static Modulus of Elasticity and Poisson's Ratio of Concrete in Compression," in *Annual Book of ASTM Standards*, ed. Philadelphia: American Society of Testing and Materials, 2010, pp. 255-258.

ASTM C39, "Standard test method for compressive strength of cylindrical concrete specimens," in *Annual Book of ASTM Standards*, ed. Philadelphia: American Society of Testing and Materials, 2001.

Aïtcin PC, Mehta PK. Effect of coarse aggregate characteristics on mechanical properties of high-strength concrete. *Materials Journal* 1990; 87(2):103-107.

Basheer L, Basheer P, Long A. Influence of coarse aggregate on the permeation, durability and the microstructure characteristics of ordinary Portland cement concrete. *Construction and Building Materials* 2005; 19(9):682-690.

Barr B, Hasso E, Weiss V. Effect of specimen and aggregate sizes upon the fracture characteristics of concrete. *International Journal of Cement Composites and Lightweight Concrete* 1986; 8(2):109-119.

Bažant ZP, Planas J. *Fracture and size effect in concrete and other quasibrittle materials*. Boca Raton: CRC press, 1998.

Bažant ZP, and Pfeiffer PA. 1987 Determination of Fracture Energy from Size Effect and Brittleness Number. *ACI Materials Journal* 1987; 84(6): 463-480.

Bažant ZP, Ožbolt J, Eligehausen R. 1994 Fracture Size Effect: Review of Evidence for Concrete Structures. *Journal of Structural Engineering* 1994; 120(8):2377.

Bažant ZP, Kazemi MT. Determination of fracture energy, process zone length and brittleness number from size effect, with application to rock and concrete. *International Journal of Fracture* 1990; 44(2):111-131.

Bažant ZP. Size effect in blunt fracture: concrete, rock, metal. *Journal of engineering mechanics* 1984; 110(4):518-535.

Bažant ZP, Kazemi MT, Hasegawa T, Mazars J. Size effect in Brazilian split-cylinder tests. *Measurements and fracture analysis. ACI Materials Journal* 1991; 88(3):325-332.

Beygi MH, Kazemi MT, Nikbin IM, Amiri JV, Rabbanifar S, Rahmani E. The influence of coarse aggregate size and volume on the fracture behavior and brittleness of self-compacting concrete. *Cement and Concrete Research* 2014; 66:75-90.

Chen B, Liu J. Investigation of effects of aggregate size on the fracture behavior of high performance concrete by acoustic emission. *Construction and Building Materials* 2007; 21(8):1696-1701.

Chen B, Liu JY. Effect of aggregate on the fracture behavior of high strength concrete. *Construction and Building Materials* 2004; 18(8):585-590.

Coopamootoo K, Masoero E. Cement pastes with UV-irradiated polypropylene: Fracture energy and the benefit of adding metakaolin. *Construction and Building Materials* 2018; 165:303-309.

Das S, Aguayo M, Sant G, Mobasher B, Neithalath N. Fracture process zone and tensile behavior of blended binders containing limestone powder. *Cement and Concrete Research* 2015; 73: 51-62.

Donza H, Cabrera O, Irassar E. High-strength concrete with different fine aggregate. *Cement and Concrete Research* 2002; 32(11):1755-1761.

Duan K, Hu X, Wittmann FH. Size effect on specific fracture energy of concrete. *Engineering Fracture Mechanics* 2007; 74(1-2):87-96.

Elices M, Rocco CG . Effect of aggregate size on the fracture and mechanical properties of a simple concrete. *Engineering Fracture Mechanics* 2008; 75:3839-3851.

Goble CF, Cohen MD. Influence of aggregate surface area on mechanical properties of mortar. *Materials Journal* 1999; 96(6):657-662.

Grassl P, Wong HS, Buenfeld NR. Influence of aggregate size and volume fraction on shrinkage induced micro-cracking of concrete and mortar. *Cement and Concrete Research* 2010; 40(1):85-93.

Grégoire D, Rojas-Solano LB, Pijaudier-Cabot G. Failure and size effect for notched

and unnotched concrete beams. *International Journal for Numerical and Analytical Methods in Geomechanics* 2013; 37(10):1434-1452.

Hoover CG, Bažant ZP, Vorel J, Wendner R, Hubler MH. Comprehensive concrete fracture tests: description and results. *Engineering Fracture Mechanics* 2013; 114:92-103.

Hillerborg A. Results of three comparative test series for determining the fracture energy  $G_F$  of concrete. *Materials and Structures* 1985; 18(5):407-413.

Hillerborg A, Modeer M, Petersson PE. Analysis of crack formation and crack growth in concrete by means of fracture mechanics and finite elements. *Cement and Concrete Research* 1976; 6:773-782.

Issa MA, Issa MA, Islam MS, Chudnovsky A. Size effects in concrete fracture—Part II: Analysis of test results. *International Journal of Fracture* 2000; 102(1):25-42.

Issa MA, Issa MA, Islam MS, Chudnovsky A. Size effects in concrete fracture: Part I, experimental setup and observations. *International Journal of Fracture* 2000; 102(1):1-24.

Jenq Y, Shah S. A fracture toughness criterion for concrete. *Engineering Fracture Mechanics* 1985; 21(5):1055-1069.

Karihaloo BL, Abdalla HM, Xiao QZ. Size effect in concrete beams. *Engineering Fracture Mechanics* 2003; 70(7-8):979-993.

Karihaloo BL, Abdalla HM, Xiao QZ. Deterministic size effect in the strength of cracked concrete structures. *Cement and Concrete Research* 2006; 36(1):171-188.

Kleinschrodt H, Winkler H. The influence of the maximum aggregate size and the size of specimen on fracture mechanics parameters. Fracture toughness and fracture energy of concrete. Ed. Wittmann FH Elsevier Science Publisher Amsterdam 1986; pp. 391-402.

Karamloo M, Mazloom M, Payganeh G. Effects of maximum aggregate size on fracture behaviors of self-compacting lightweight concrete. *Construction and Building Materials* 2016; 123:508-515.

Luković M, Schlangen E, Ye G. Combined experimental and numerical study of fracture behaviour of cement paste at the microlevel. *Cement and Concrete Research* 2015; 73:123-135.

Morel S. R-curve and size effect in quasibrittle fractures: Case of notched structures.

International Journal of Solids and Structures 2007; 44(13)4272-4290.

Mihashi H, Nomura N. Correlation between characteristics of fracture process zone and tension-softening properties of concrete. Nuclear engineering and design 1996; 165(3):359-376.

Nallathambi P, Karihaloo B, Heaton B. Effect of specimen and crack sizes, water/cement ratio and coarse aggregate texture upon fracture toughness of concrete. Magazine of Concrete Research 1984; 36(129):227-236.

Nallathambi P, Karihaloo BL, BS Heaton. Various size effects in fracture of concrete. Cement and Concrete Research 1985; 15:117-126.

Neville AM. Properties of Concrete. Pearson, Harlow, England; New York, NY, U.S. (2011)

Otsuka K, Date H. Fracture process zone in concrete tension specimen. Engineering fracture mechanics 2000; 65(2):111-131.

Petersson P. Fracture energy of concrete: practical performance and experimental results. Cement and Concrete Research 1980; 10(1):91-101.

Regnault P, Brühwiler E. Holographic interferometry for the determination of fracture process zone in concrete. Engineering fracture mechanics 1990; 35(1-3):29-38.

RILEM Recommendation. Fracture Mechanics of Concrete-Test Methods, Size effect method for determining fracture energy and process zone size of concrete. Materials and Structures 1990; 23:461-465.

Rao GA, Prasad BR. Fracture energy and softening behavior of high-strength concrete. Cement and Concrete Research 2002; 32(2):247-252.

Trunk B, Wittmann FH. Experimental investigation into the size dependence of fracture mechanics parameters. In: Proceedings of 3rd International Conference Fracture Mechanics Concrete Structures, 1998, pp. 1937-1948.

Tasdemir C, Tasdemir MA, Mills N, Barr BI, Lydon FD. Combined Effects of Silica Fume, Aggregate Type, and Size on Post-Peak Response of Concrete in Bending. Materials Journal 1999; 96(1):74-83.

Van Vliet MRA, Van Mier JGM. Experimental investigation of size effect in concrete and sandstone under uniaxial tension. Engineering Fracture Mechanics 2000; 65(2-3):165-188.

Wu KR, Chen B, Yao W, Zhang D. Effect of coarse aggregate type on mechanical properties of high-performance concrete. *Cement and Concrete Research* 2001a; 31(10):1421-1425.

Wu K, Chen B, Yao W. Study of the influence of aggregate size distribution on mechanical properties of concrete by acoustic emission technique. *Cement and Concrete Research* 2001b; 31(6):919-923.

Wolinski S, Hordijk DA, Reinhardt HW, Cornelissen HA. Influence of aggregate size on fracture mechanics parameters of concrete. *International Journal of Cement Composites and Lightweight Concrete* 1987; 9(2):95-103.

Xu S, Zhu Y. Experimental determination of fracture parameters for crack propagation in hardening cement paste and mortar. *International Journal of Fracture* 2009; 157(1-2):33-43.

Zhao Z, Kwon SH, Shah SP. Effect of specimen size on fracture energy and softening curve of concrete: Part I. Experiments and fracture energy. *Cement and Concrete Research* 2008; 38(8):1049-1060.